Magnetic Properties of Manganese in the Photosynthetic O_2-Evolving Complex. 2. Evidence for a Manganese Tetramer

Julio C. de Paula, Warren F. Beck, and Gary W. Brudvig*

Contribution from the Department of Chemistry, Yale University, New Haven, Connecticut 06511. *Received December 30, 1985*

Abstract: Five distinct EPR signals which originate from the S_2 state of the O_2-evolving complex of photosystem II are generated by low-temperature illumination and observed at liquid helium temperatures. The magnetic properties of these five S_2 state species are interpreted in terms of a model consisting of an exchange coupled Mn tetramer, where both ferromagnetic and antiferromagnetic exchange occur simultaneously to give an $s = {}^3/_2$ ground state and an $s = {}^1/_2$ first excited state. The multiline EPR signals from the S_2 state of resting, active, and NH_4Cl-treated photosystem II membranes are proposed to arise from the excited $s = {}^1/_2$ state. The different magnetic properties of these S_2 state species are explained by changes in the exchange coupling constants which modulate the energy spacing between the ground $s = {}^3/_2$ state and the excited $s = {}^1/_2$ state. The $g = 4.1$ S_2 state EPR signal exhibits Curie behavior in the 4.0–25.0 K range and is proposed to arise from the $s = {}^3/_2$ ground state of the Mn complex, in a configuration where the $s = {}^1/_2$ excited state is thermally inaccessible. The Mn tetramer model is successful in predicting the ^{55}Mn nuclear hyperfine interaction in the S_2 state multiline EPR spectrum from untreated resting state samples and also the reduced ^{55}Mn nuclear hyperfine coupling in the S_2 state multiline EPR spectrum from NH_4Cl-treated samples relative to untreated resting state samples. The combination of ferromagnetic and antiferromagnetic exchange coupling in the Mn site of the O_2-evolving complex is analogous to the case encountered in Fe_4S_4 proteins and Cu_4O_4 cubane-like complexes. On the basis of this analogy, we postulate a Mn_4O_4 cubane-like structure for the active site of water oxidation in the S_2 state.

The photooxidation of H_2O to O_2 in the O_2-evolving complex (OEC) of photosystem II (PSII) occurs via the formation of five intermediate oxidation states known as S_i ($i = 0$ to 4) states.[1] It has long been known that Mn is required for O_2 evolution (reviewed in ref 2), and it has been found that four Mn ions are present in the OEC.[3] A Mn complex appears to be the site at which oxidizing equivalents are stored during S-state transitions and also the site where water oxidation occurs. Until recently, however, very little information has been gathered about the structure and ligand binding properties of the Mn site of the OEC.

We have characterized five distinct EPR signals from the S_2 state of the OEC,[4-7] which are generated by a one-electron photooxidation of the dark-stable S_1 state at temperatures ranging from 140 to 273 K. Long-term dark-incubated, or resting state, PSII membranes which are illuminated at 200 K exhibit the S_2 state multiline EPR signal first reported by Dismukes and Siderer.[8] Illumination of resting state PSII membranes at 130 K produces an S_2 state EPR signal with a single 250-G-wide turning point at $g = 4.1$.[4,9,10] This $g = 4.1$ EPR signal is replaced by the multiline EPR signal upon incubation at 200 K in the dark. From studies of the one and two electron transfer steps in PSII membranes at cryogenic temperatures, we concluded that both the $g = 4.1$ and the multiline EPR signals originate from the same paramagnetic site in the S_2 state;[4] this interpretation has subsequently been supported by ligand-binding studies.[11] The differences between the two spectroscopic forms of the S_2 state were proposed to arise from a structural change which is dependent on the temperature. In contrast to the long-term dark-adapted, resting state case, short-term dark-adapted, or active state, PSII membranes exhibit two distinct S_2 state multiline EPR signals, generated by illumination at 160 and 170 K. These two S_2 state multiline EPR signals differ from the resting state multiline EPR signal both in their hyperfine splitting patterns and in their magnetic properties.[5,6] More recently, Beck et al.[7] have shown that PSII membrane samples which are treated with 100 mM NH_4Cl exhibit a perturbed S_2 state multiline EPR signal with considerably smaller hyperfine splittings than those in the untreated resting state samples. It was concluded that the perturbed S_2 state EPR signal was due to the direct binding of ammonia to the Mn site of the OEC.

Our investigation of the magnetic properties of the S_2 state multiline EPR signals in both the active and resting states[6] has established that these EPR signals arise from an $s = {}^1/_2$ excited spin state of an exchange-coupled Mn complex which has an $s = {}^3/_2$ ground state. At the time these results were published, we proposed a simple model for the S_2 state of the OEC which consisted of a trimer of Mn^{III}, Mn^{IV}, and another $s = 1$ species, which could not be identified in our earlier studies.

In this contribution, we provide a more complete interpretation of the earlier EPR data and include new experimental data on the magnetic properties of the $g = 4.1$ S_2 state EPR signal and the S_2 state multiline EPR signal produced by 245 K illumination in active state samples. We also present an interpretation of the temperature-dependence data of the S_2 state EPR signal from NH_4Cl-treated PSII membranes. These data can be best explained by a model of the S_2 state which consists of a mixed-valence manganese tetramer. Full matrix spin Hamiltonian calculations show that both ferromagnetic and antiferromagnetic exchange couplings between the Mn ions must be invoked in order to explain the data. This model can account for the different magnetic properties of the five S_2 state species by varying the exchange coupling constants. Moreover, the combination of ferromagnetic and antiferromagnetic exchange coupling in a Mn tetramer, required to account for the magnetic properties of the S_2 state, is quite analogous to that found in Fe_4S_4 proteins[12] and also in Cu_4O_4 cubane-like complexes.[13] This analogy suggests

(1) Kok, B.; Forbush, B.; McGloin, M. *Photochem. Photobiol.* **1970**, *11*, 457.
(2) Amesz, J. *Biochim. Biophys. Acta* **1983**, *726*, 1.
(3) Murata, N.; Miyao, M.; Omata, T.; Matsunami, H.; Kubawara, T. *Biochim. Biophys. Acta* **1984**, *765*, 363.
(4) de Paula, J. C.; Innes, J. B.; Brudvig, G. W. *Biochemistry* **1985**, *24*, 8114.
(5) Beck, W. F.; de Paula, J. C.; Brudvig, G. W. *Biochemistry* **1985**, *24*, 3035.
(6) de Paula, J. C.; Brudvig, G. W. *J. Am. Chem. Soc.* **1985**, *107*, 2643.
(7) Beck, W. F.; de Paula, J. C.; Brudvig, G. W., *J. Am. Chem. Soc.*, in press.
(8) Dismukes, G. C.; Siderer, Y. *Proc. Natl. Acad. Sci. U.S.A.* **1981**, *78*, 724.
(9) Casey, J. L.; Sauer, K. *Biochim. Biophys. Acta* **1984**, *767*, 21.
(10) Zimmermann, J. L.; Rutherford, A. W. *Biochim. Biophys. Acta* **1984**, *767*, 160.
(11) Beck, W. F.; Brudvig, G. W. *Biochemistry*, in press.
(12) (a) Noodleman, L.; Norman, J. G., Jr.; Osborne, J. H.; Aizman, A.; Case, D. A. *J. Am. Chem. Soc.* **1985**, *107*, 3418. (b) Cammack, R.; Dickson, D. P. E.; Johnson, C. E. *Iron-Sulfur Proteins*; Lovenberg, W., Ed.; Academic Press: New York, 1977; Vol. 3, p 283.

0002-7863/86/1508-4002$01.50/0

a Mn_4O_4 cubane-like structure for the active site of water oxidation in the S_2 state.

Experimental Section

The preparation of PSII membranes and the method for the generation of S_2 state EPR signals have been described elsewhere.[4,5] The temperature dependence and power saturation studies were carried out as in ref 6, and the protocol for NH_4Cl treatment of PSII membranes was that of ref 7. All calculations were performed with a VAX 11/750 computer with EISPAK routines for matrix diagonalization.

Theory

Temperature-Dependence Studies. The S_2 state multiline EPR signal was the first spectroscopic probe of the OEC that contained a considerable amount of structural information. As a consequence, much effort has been made to translate this information into a structural model of the metal-containing site of the OEC. The first proposals involved antiferromagnetically exchange coupled mixed-valence Mn dimers or tetramers,[8,14,15] but computer simulations of the S_2 state multiline EPR spectrum using these models could not completely explain several of the spectral features, such as the number of hyperfine lines and their intensity pattern. Furthermore, a single dimer of Mn could not explain the temperature dependence of the S_2 state multiline EPR signal.[6] Therefore, a third paramagnetic site, which could be either an $s = 1$ paramagnet or another Mn dimer, was proposed to be ferromagnetically coupled to a Mn^{III}–Mn^{IV} dimer in the S_2 state.[6] We have investigated the possibility that an $s = 1$ ion, such as low-spin Fe^{IV}, is ferromagnetically exchange coupled to an antiferromagnetically exchange coupled Mn^{III}–Mn^{IV} dimer. In such a trimeric system, the ^{55}Mn nuclear hyperfine interaction will be reduced significantly. This happens because the Fe^{IV} ion ($I = 0$) does not contribute to the nuclear hyperfine interaction but does influence the total spin of the system. Therefore, the projections of the nuclear hyperfine tensors of the individual Mn ions onto the trimer spin are decreased when compared to the Mn dimer case. In order to compensate for this lowering of the projection of the Mn nuclear hyperfine tensor, an unreasonably large increase in the free ion nuclear hyperfine coupling constant must be invoked. An accurate simulation of the hyperfine structure of the S_2 state multiline EPR signal using this trimer model requires that the ^{55}Mn nuclear hyperfine coupling constants for the Mn ions be set at values which exceed those expected from the purely ionic case. It is unlikely, therefore, that an $s = 1$ ion constitutes the third paramagnetic site which must be exchange coupled to a Mn dimer in order to explain the magnetic properties of the S_2 state of the OEC.

The available data on the chemical composition of PSII membrane preparations show that four Mn ions per OEC are required for O_2 evolution.[3] It is reasonable, therefore, to propose a model for the catalytic site of the OEC which consists of a tetramer of Mn incorporating the conclusions drawn from the magnetic data. The oxidation states of Mn in the OEC can be estimated from the X-ray absorption data of Goodin et al.[16] These studies indicate that both Mn^{III} and Mn^{IV} are present in the S_2 state of the OEC. We have, therefore, chosen a model for the S_2 state of the OEC consisting of three Mn^{III} ions ($s_1 = s_2 = s_3 = 2$) and one Mn^{IV} ion ($s_4 = {}^3/_2$).[17] The zero-field spin Hamiltonian which we have used to describe this model is given by

$$\hat{H}_{zf} = \sum_{i<k} J_{ik}\hat{s}_i\hat{s}_k + \sum_i D_i[\hat{s}_{iz}^2 - {}^1/_3 s_i(s_i + 1)] \qquad (1)$$

where $\hat{s}_i$ and $\hat{s}_k$ are the electron spin operators, J_{ik} is the isotropic superexchange coupling constant between ions i and k, and D_i is the spin–spin coupling constant for each Mn ion. As we have written the superexchange interaction, antiferromagnetic exchange arises if $J_{ik} > 0$, and ferromagnetic exchange is present if $J_{ik} < 0$. The zero-field Hamiltonian for a $3Mn^{III}$–Mn^{IV} tetramer (given by eq 1) is described by a 500×500 matrix. In order to obtain the energy levels, one simply needs to diagonalize $\hat{H}_{zf}$. The eigenvalues can then be used to simulate the temperature dependence of the EPR signal intensity.

The temperature dependence of the intensity, $I(T)$, of an $m_s = -{}^1/_2 \leftrightarrow m_s = +{}^1/_2$ EPR transition in the limit where $kT \gg h\nu$ is given by

$$I(T) = (K/T)[1/\sum_i N_i \exp(-W_i/kT)] \qquad (2)$$

where ν is the microwave frequency for the EPR measurement, h is Planck's constant, K is a proportionality constant, k is the Boltzmann constant, and W_i are the zero-field energies of the spin levels with degeneracies N_i, obtained by diagonalization of $\hat{H}_{zf}$. In some of our energy level calculations the full 500×500 matrix was diagonalized in order to allow variation of all J_{ik}'s and D_i's independently, thereby assuming no special symmetry in the tetramer. For our initial calculations, the energy levels were obtained by full-matrix diagonalization for a range of J_{ik}'s and D_i's. These calculations established the combination of J_{ik}'s necessary to generate an $s = {}^3/_2$ ground state and an $s = {}^1/_2$ first excited state (as dictated by the analysis in ref 6). It was found that it is possible to generate an $s = {}^3/_2$ ground state and an $s = {}^1/_2$ first excited state for an exchange-coupled $3Mn^{III}$–Mn^{IV} system, but only with a rather restricted combination of exchange couplings. The required combination of exchange couplings is as follows: (i) a large antiferromagnetic exchange coupling between a Mn^{III}–Mn^{IV} pair; (ii) a smaller antiferromagnetic exchange coupling between the remaining Mn^{III}–Mn^{III} pair; and (iii) all remaining interactions being ferromagnetic.

It is possible to simplify this calculation, however, when one of the terms in $\hat{H}_{zf}$ is large. If we allow a dimer of Mn^{III}–Mn^{IV} to be very strongly antiferromagnetically exchange coupled, then only its $s = {}^1/_2$ ground spin state need be considered when the weaker exchange couplings with the other two Mn^{III} ions are included. This reduces the problem to a trimer of $s_1 = s_2 = 2$ and $s_D = {}^1/_2$, which can be described by a 50×50 Hamiltonian matrix, where s_D is the ground state of the antiferromagnetically exchange coupled Mn^{III}–Mn^{IV} dimer. This simplification introduces no error in the ordering and relative energies of the lowest energy spin levels, provided that a sufficiently large value for the antiferromagnetic exchange coupling constant is chosen, and greatly reduces the computational time.

In order to gain more insight into the types of coupling schemes which are necessary to arrive at an $s = {}^3/_2$ ground state and an $s = {}^1/_2$ first excited state, let us simplify the problem so that the exchange Hamiltonian becomes diagonal. According to Sinn,[18] this can be achieved by letting $J' = J_{1D} = J_{2D}$ and $\bar{s}' = \bar{s}_1 + \bar{s}_2$, where the coefficients 1, 2, and D refer to Mn ion 1 ($s_1 = 2$), Mn ion 2 ($s_2 = 2$), and the Mn^{III}–Mn^{IV} dimer ($s_D = {}^1/_2$), respectively. Let $J = J_{12}$ and $\bar{s} = \bar{s}' + \bar{s}_D$, then the energy levels $E(s,s')$ are given by

$$E(s,s') = {}^1/_2(J - J')[s'(s'+1) - s_1(s_1+1) - s_2(s_2+1)] + {}^1/_2 J'[s(s+1) - s_1(s_1+1) - s_2(s_2+1) - s_D(s_D+1)] = {}^1/_2(J - J')[s'(s'+1) - 12] + {}^1/_2 J'[s(s+1) - 51/4] \qquad (3)$$

Figure 1 displays the energy levels $E(s,s')$ for several combinations of J and J'. It is clear that, in order to obtain an ($s = {}^3/_2, s' = 1$) ground state and an ($s = {}^1/_2, s' = 0$) first excited state, J must be positive (antiferromagnetic exchange) and J' negative (ferromagnetic exchange). Furthermore, the following condition must apply: $2|J| < |J'| < 3|J|$. Note that the antiferromagnetic exchange coupling between the Mn^{III}–Mn^{IV} pair must be large

(13) Haase, W.; Walz, L.; Nepveu, F. *The Coordination Chemistry of Metalloenzymes*; Bertini, I. et al., Eds.; D. Reidel Publishing Co.: Dordrecht, Holland, 1983; p 229.
(14) Hansson, Ö.; Andréasson, L.-E. *Biochim. Biophys. Acta* **1982**, *679*, 621.
(15) Dismukes, G. C.; Ferris, K.; Watnick, P. *Photobiochem. Photobiophys.* **1982**, *3*, 243.
(16) Goodin, D. B.; Yachandra, V. K.; Britt, R. D.; Sauer, K.; Klein, M. P. *Biochim. Biophys. Acta* **1984**, *767*, 209.
(17) Although we present explicit calculations only for the $3Mn^{III}$–Mn^{IV} case, calculations done for either a $3Mn^{III}$–Mn^{II} or $3Mn^{IV}$–Mn^{III} model give equivalent results. The EPR spectral analyses that we present, therefore, cannot discriminate between these three possible oxidation states of a manganese tetramer.
(18) Sinn, E. *Coord. Chem. Rev.* **1970**, *5*, 313.

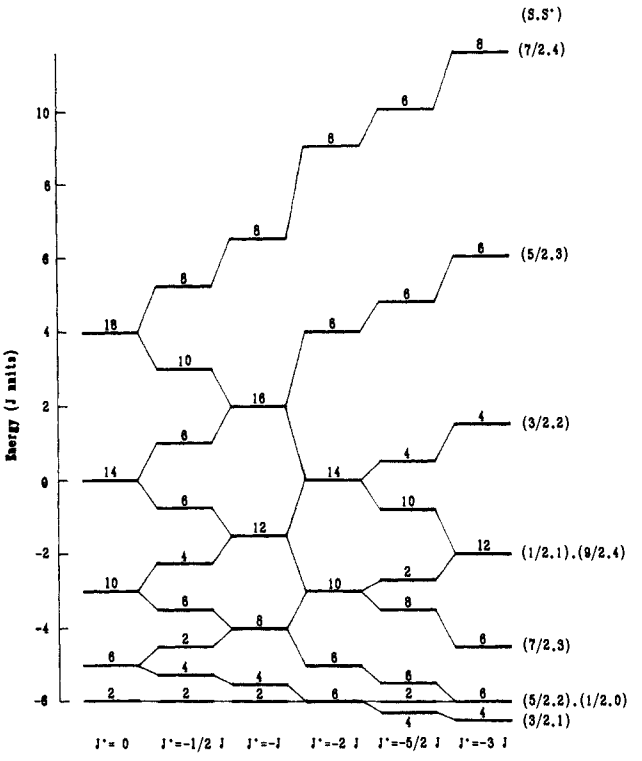

Figure 1. Energy level diagrams for several exchange coupling schemes of a $3Mn^{III}$–Mn^{IV} tetramer. The Hamiltonian is given by eq 1 of the text and the energies are given in eq 3. The number placed on top of each level denotes its degeneracy, given by $N_i = 2s_i + 1$.

relative to either $|J|$ or $|J'|$ in this approximation.

Hyperfine Reduction Constants. In an attempt to understand the ^{55}Mn nuclear hyperfine interactions in the S_2 state multiline EPR signals, we have also determined the projection of the nuclear hyperfine coupling tensors of each individual ion on the total tetramer spin. If s and s' are good quantum numbers, this calculation can be performed by using vector coupling rules.[19] For cases where s is not a good quantum number, as in the present case, the hyperfine reduction constants of each ion can be calculated by first diagonalizing the approximate zero-field Hamiltonian (given by eq 1 with $s_1 = s_2 = 2$ and $s_D = {}^1/_2$) and then obtaining the eigenfunctions $Y_{\pm 1/2} = \sum_i a_i \phi_i$ corresponding to the $m_s = \pm {}^1/_2$ levels of the ($s = {}^1/_2$, $s' = 0$) Kramer's doublet from which the EPR transition arises, where ϕ_i are the basis functions used to generate the Hamiltonian matrix. We set up our calculation using the uncoupled representation in which the basis functions are $|s_1\, s_2\, s_D\, m_1\, m_2\, m_D\rangle$. The first-order corrections to the zero-field energies brought about by nuclear hyperfine interactions will be

$$\langle Y_{\pm 1/2}|\sum_j A_j \hat{s}_{jz}\hat{i}_{jz}|Y_{\pm 1/2}\rangle = \sum_j [A_j m_{Ij}(\sum_i m_{Ji} a_i^2)] \quad (4)$$

where A_j is the isotropic nuclear hyperfine coupling constant of the jth ion, $\hat{s}_{jz}$ is the z component of the electron spin operator of the jth ion, $\hat{i}_{jz}$ is the z component of the nuclear spin operator of the jth ion, and m_{Ij} is the z projection of the nuclear spin of the jth ion. The constants $c_j = \sum_i m_{Ji} a_i^2$ determine the projection of the each Mn ion's nuclear hyperfine coupling in the tetramer.

We must remember that s_D actually represents the ground state of a Mn^{III}–Mn^{IV} dimer. The nuclear hyperfine reduction constants for the Mn^{III} and Mn^{IV} ions of this dimer, which we will call c_3 and c_4, respectively, can be calculated from vector coupling rules, and the results have been given by Hansson and Andréasson:[14]

$$\mathbf{A}_{dimer} = 2\mathbf{A}_{Mn(III)} - \mathbf{A}_{Mn(IV)} \quad (5)$$

Therefore, $c_3 = 2c_D$ and $c_4 = -c_D$.

(19) Scaringe, R. P.; Hodgson, D. J.; Hatfield, W. E. *Mol. Phys.* **1978**, *35*, 701.

EPR Spectral Simulations. It will be seen that in the resting S_2 state multiline EPR signal the ^{55}Mn nuclear hyperfine interactions for a Mn tetramer can be closely approximated by a Mn^{III}–Mn^{IV} dimer model, since the value of c_D was close to unity and the values of c_1 and c_2 were close to zero, in that case (Table II). Hence, it should be possible to simulate the resting S_2 state multiline EPR signal by using the much simpler model consisting of a strongly antiferromagnetically exchange-coupled Mn^{III}–Mn^{IV} dimer. We have followed the procedures outlined by Hansson and Andréasson,[14] except that, in certain cases, anisotropy was included in the **g** tensor. If we let $\mathbf{g}_1$, $\mathbf{g}_2$, $\mathbf{A}_1'$, and $\mathbf{A}_2'$ be the single ion **g** and **A** tensors, respectively, the dimer tensors $\mathbf{g}^c$ and $\mathbf{A}_i^c$ can be defined in terms of the constant

$$C = [s_1(s_1 + 1) - s_2(s_2 + 1)]/s(s + 1) \quad (6)$$

so that,

$$\mathbf{g}^c = [(1 + C)/2]\mathbf{g}_1 + [(1 - C)/2]\mathbf{g}_2 \quad (7)$$

$$\mathbf{A}_1^c = [(1 + C)/2]\mathbf{A}_1' \quad (8)$$

$$\mathbf{A}_2^c = [(1 - C)/2]\mathbf{A}_2' \quad (9)$$

The resonance condition is, then, given by

$$h\nu = \beta HG + m_{I1}A_1^c + m_{I2}A_2^c + [(A_1^c)^2(I_1(I_1 + 1) - m_{I1}^2) + {}^1/_4(A_2^c)^2(I_2(I_2 + 1) - m_{2I}^2)]/\beta HG \quad (10)$$

where we have assumed isotropic nuclear hyperfine coupling interactions for each Mn ion. The G term is a constant if the **g** tensor is assumed to be isotropic; if an anisotropic **g** tensor is used in the calculation, G is written in terms of the parameters

$$c_{ix} = {}^1/_2 g_{ix} \sin\theta \cos\phi \quad (11a)$$

$$c_{iy} = -{}^1/_2 g_{iy} \sin\theta \sin\phi \quad (11b)$$

$$c_{iz} = g_{iz} \cos\theta \quad (11c)$$

The angles θ and ϕ of eq 11 define the direction of the magnetic field relative to the molecular principal axes. The term G can then be written as

$$G = 2[(c_{1z} - {}^1/_2 c_{2z})^2 + 4(c_{1x}^2 - c_{1x}c_{2x} + c_{1y}^2 - c_{1y}c_{2y}) + c_{2x}^2 + c_{2y}^2]^{1/2} \quad (12)$$

A computer program was written to simulate spectra for a Mn^{III}–Mn^{IV} dimer. The resonant field was determined by using eq 10, and a Gaussian line shape was introduced at each resonant field position. The simulations in this paper required 30 increments of both θ and ϕ to achieve convergence.

Results and Discussion

Temperature Dependence of the S_2 State EPR Signals. Our previous study of the magnetic properties of the active and resting S_2 state species established that the multiline EPR signals arise from an $s = {}^1/_2$ excited spin state of a metal complex which has an $s = {}^3/_2$ ground state.[6] These conclusions were drawn from the simulation of the temperature-dependence curves of the EPR signals in question. In summary, we found that the intensity of the resting S_2 state multiline EPR signal (Figure 2a) in the 3.7–25.0 K range exhibited a maximum at 6.9 K under nonsaturating conditions (Figure 3a), a behavior characteristic of an EPR transition which arises from an excited spin state. Similarly, the active S_2 state multiline EPR signal generated by 170 K illumination also exhibited an intensity maximum, but at 5.9 K (data for an equivalent state produced by 245 K illumination are shown in Figures 2e and 4b). In contrast, the active S_2 state multiline EPR signal produced by 160 K illumination (Figure 2d) exhibited Curie behavior in the 4.5–20.0 K range (Figure 4a). This temperature dependence was ascribed to an EPR transition within an $s = {}^1/_2$ excited spin state which is less than 2.9 cm^{-1} above the ground state, such that the system was in the high-temperature limit above 4 K.

We present the magnetic properties of two additional EPR signals from the resting S_2 state of the OEC. These include the $g = 4.1$ EPR signal produced by 130 K illumination and the S_2

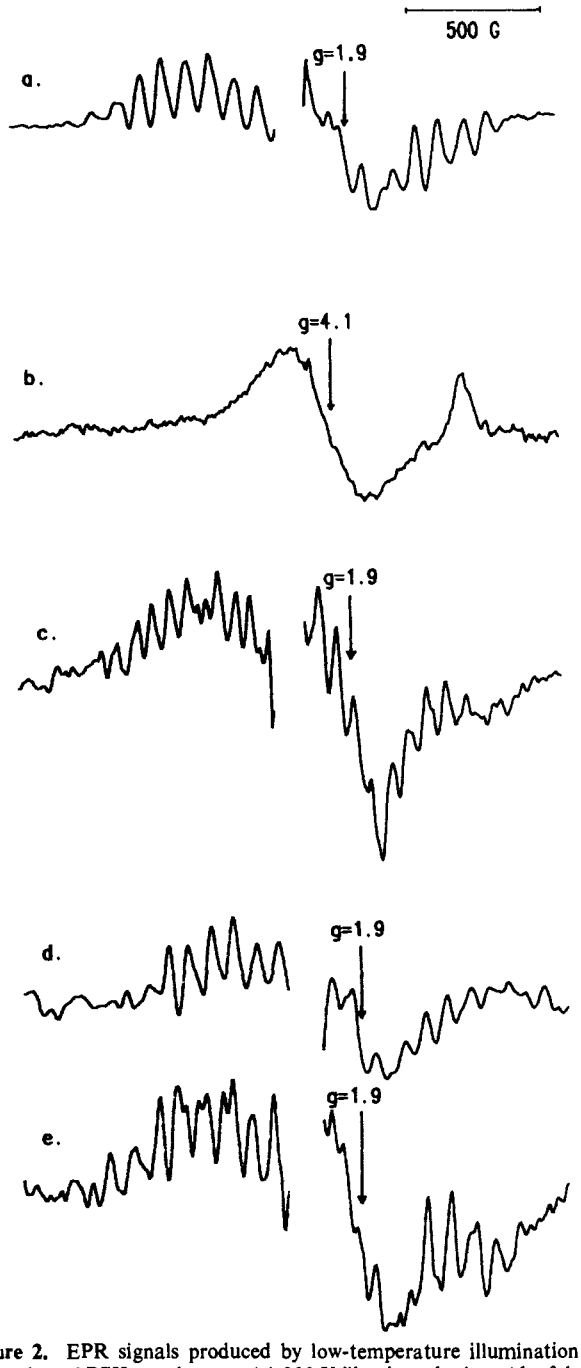

Figure 2. EPR signals produced by low-temperature illumination of dark-adapted PSII membranes: (a) 200 K illuminated minus 4 h of dark; (b) 130 K illuminated minus 4 h of dark; (c) 0 °C illuminated minus 4 h of dark PSII membranes treated with 100 mM NH_4Cl; (d) 160 K illuminated minus 6 min of dark; (e) 245 K illuminated minus 6 min of dark. Instrument conditions: microwave power, 0.2 mW; modulation frequency, 100 KHz; modulation amplitude, 20 G; microwave frequency, 9.10 GHz; sample temperature, 7 K (a, c, d, e) or 10 K (b).

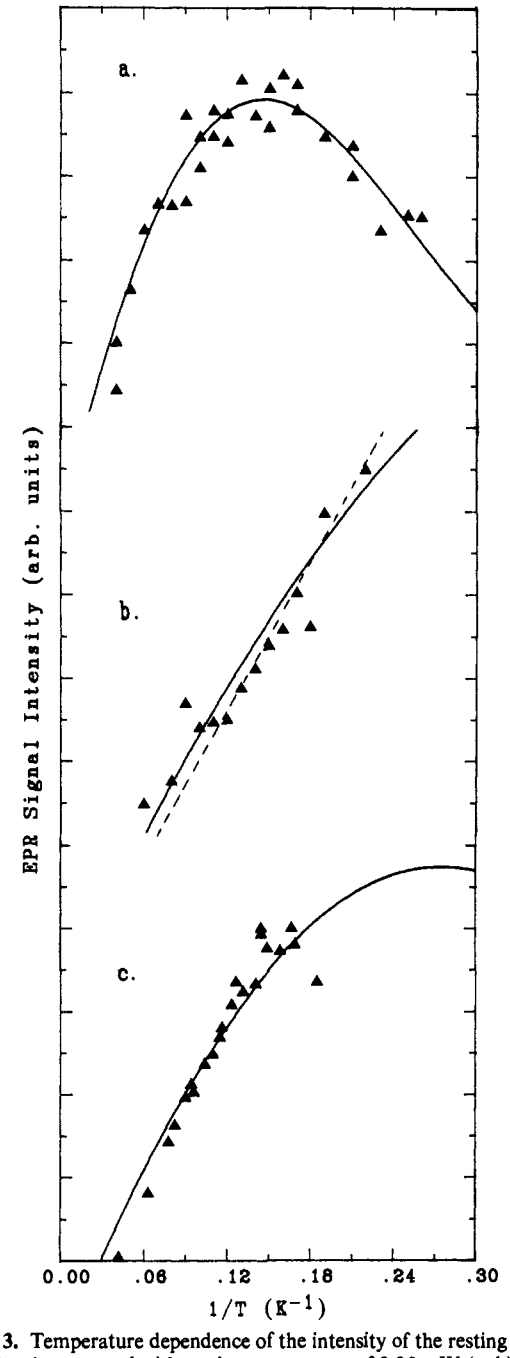

Figure 3. Temperature dependence of the intensity of the resting S_2 state EPR signals measured with a microwave power of 0.05 mW (a, b) or 0.02 mW (c). The lines through the data are computer fits to eq 2 of the text with the energy levels obtained by diagonalization of $\hat{H}_{zf}$ and using the parameters of Table I. (a) Untreated sample illuminated at 200 K; (b) untreated sample illuminated at 130 K (for the dotted line, $D = 2.0$ cm^{-1}, for the solid line, $D = -1.0$ cm^{-1}); (c) sample treated with 100 mM NH_4Cl and illuminated at 0 °C. Signal intensities were determined as peak-to-peak heights; for the multiline signals, three peaks to high-field and three peaks to low-field of $g = 2.0$ were added together. Each plot was arbitrarily offset along the y axis. Spectrometer conditions as in Figure 2.

state multiline EPR signal obtained by 0 °C illumination of 100 mM NH_4Cl-treated samples (Figure 2, parts b and c, respectively). The latter differs from the untreated case in that the individual hyperfine lines are separated by an average of 67.5 G, and not 87 G. We also present new data on the S_2 state multiline EPR signal generated by 245 K illumination of active state PSII membranes which were treated with 75 μM 3-(3,4-dichlorophenyl)-1,1-dimethylurea (DCMU) to limit the OEC to a single turnover (Figure 2e). The S_2 state species produced in active state samples by illumination at 245 K is equivalent to that produced by illumination at 170 K (as in our previous study[6]), although this S_2 state species is produced more reproducibly at 245 K.

The $g = 4.1$ S_2 state EPR signal shows Curie behavior in the 4.0–20.0 K range (Figure 3b). At 5.0 K, this signal could not be saturated ($P_{1/2} > 156$ mW). The temperature-dependence result can be interpreted in terms of a ground spin state giving rise to the spectrum or, alternatively, in terms of an excited spin state which is less than approximately 3 cm^{-1} above the ground state such that the system is in the high-temperature limit above 4 K. As described above, the $g = 4.1$ EPR signal is proposed to arise from the same site which also exhibits a multiline EPR signal. There are several assignments of the $g = 4.1$ EPR signal which are also consistent with this conclusion. We note, however, that an $s = {}^1/_2$ spin state is not expected to exhibit a turning point at $g = 4.1$. Hence, the assignment of the $g = 4.1$ EPR signal must

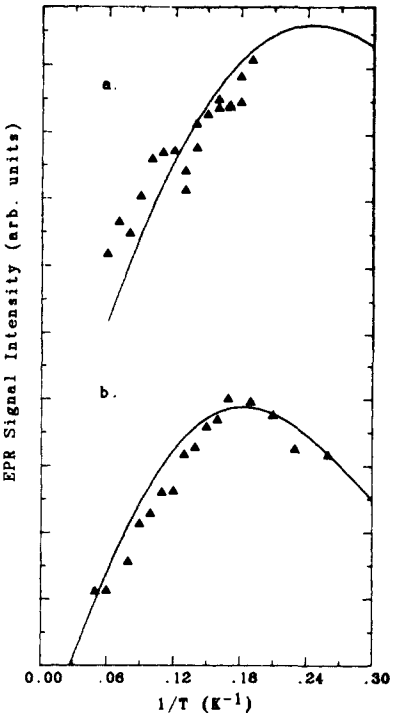

Figure 4. Temperature dependence of the intensity of the active S_2 state EPR signals measured with a microwave power of 0.05 mW: (a) untreated sample illuminated at 160 K; (b) untreated sample illuminated at 245 K. Data analysis and spectrometer conditions as in Figure 3.

differ from that of the multiline EPR signals.

Casey and Sauer[9] proposed that the $g = 4.1$ EPR signal from the OEC was due to non-heme Fe^{III} ($s = {}^5/_2$) in a rhombic environment. Indeed, a broad EPR signal at $g_y = 4.1$ due to a high-spin Fe^{III} ion is observed from the FeS center of *D. gigas* desulforedoxin.[20] This EPR feature is accompanied, however, by a turning point at $g_x = 7.7$; the splitting of the x and y components reflects the nonaxial symmetry of the FeS center. We find that a lower field turning point does not accompany the $g = 4.1$ EPR signal in 130 K illuminated resting state PSII membranes. Hence, it is unlikely that the $g = 4.1$ EPR signal arises from an $s = {}^5/_2$ ion in a rhombic environment. Moreover, the conclusion that the $g = 4.1$ EPR signal arises from the Mn site renders the assignment of this EPR signal to a Fe^{III} species unnecessary.

One attractive possibility that accounts for the Curie behavior of the $g = 4.1$ EPR signal is that it arises from the ground $s = {}^3/_2$ state predicted by our previous studies.[6] The g value of 4.1 for this EPR signal suggests that the transition arises from an $s = {}^3/_2$ state with a large axial zero-field splitting interaction. It is known that $s = {}^3/_2$ ions exhibit a turning point at $g = 4$ due to the $m_s = -{}^1/_2 \leftrightarrow m_s = +{}^1/_2$ transition, provided that $|D| \gg h\nu$ and $|E| \sim 0$.[21] Alternatively, the $g = 4.1$ EPR signal could arise from a transition between the $m_s = \pm{}^1/_2$ and $m_s = \pm{}^3/_2$ sublevels in an $s = {}^3/_2$ state, provided that $|D|$ is small. This assignment would require that $|D| \sim h\nu$ in order for a transition to be observed at $g = 4.1$ and also would make the position of the $g = 4.1$ EPR signal dependent on the magnitude of $|D|$ as well as $h\nu$. The orientation dependence of the intensity and field position of the $g = 4.1$ EPR signal suggests that this EPR signal arises from a magnetically anisotropic site.[22] This lends support to the assignments proposed above, which predict that the $g = 4.1$ EPR signal should exhibit considerable anisotropy.

Other assignments of the $g = 4.1$ EPR signal could be invoked as well, such as a transition from an $s = {}^5/_2$ state.[9] These assignments, however, seem less plausible because a very large change in the exchange coupling scheme of the Mn site would be required between 130 and 200 K in order to account for the conversion of the $g = 4.1$ EPR signal species into the multiline EPR signal species.

For the assignment of the $g = 4.1$ EPR signal to the ground $s = {}^3/_2$ state of a Mn tetramer, the change that occurs when the $g = 4.1$ EPR signal species converts into the multiline EPR signal species as the temperature is raised from 140 to 200 K would simply reflect a change in the exchange coupling constants. In the $g = 4.1$ EPR signal species, the $s = {}^1/_2$ state would be thermally inaccessible, so that only the $g = 4.1$ EPR signal from the $s = {}^3/_2$ ground state would be observed; the exchange couplings for the multiline EPR signal species would be smaller, such that the $s = {}^1/_2$ excited state is thermally accessible and gives rise to the multiline EPR signal.

Our conclusion that the $g = 4.1$ EPR signal arises from an $s = {}^3/_2$ state of the same Mn complex which gives rise to the S_2 state multiline EPR signals is strengthened by the fact that synthetic complexes of Mn^{IV} ($s = {}^3/_2$) can exhibit EPR features at $g = 4.0$. In particular, Richens and Sawyer[23] have shown that the EPR spectrum of bis(tetramethylammonium)tris(sorbitolato)manganate(IV) has a broad turning point at $g = 4.0$, characteristic of a $m_s = -{}^1/_2 \leftrightarrow m_s = +{}^1/_2$ transition with $|D| \gg h\nu$. These EPR spectra do not show resolved ^{55}Mn nuclear hyperfine couplings. It is quite reasonable, therefore, that the $g = 4.1$ S_2 state EPR signal arises from the Mn complex of the OEC.

The S_2 state multiline EPR signal obtained by 0 °C illumination of 100 mM NH_4Cl-treated PSII membranes also shows Curie behavior in the range of 5.0–25.0 K (Figure 3c). The question is then whether this EPR signal arises from an excited $s = {}^1/_2$ state as in the S_2 state multiline EPR signals from untreated samples. It is noted that the S_2 state spectrum of the ammonia-bound samples is centered at $g = 2.0$ and has a multiline hyperfine pattern which is similar, though not identical, to the resting S_2 state multiline EPR signal. It is, therefore, reasonable to conclude that the S_2 state EPR spectrum of ammonia-bound PSII membranes arises from an excited $s = {}^1/_2$ state of the Mn complex of the OEC, as does the resting S_2 state multiline EPR signal.

Theoretical Model of the S_2 State of the OEC. We propose assignments for the five S_2 state EPR signals based on an exchange-coupled Mn tetramer. These assignments have been made by invoking the minimum variation in exchange couplings required to account for the temperature dependence of the EPR signal intensities and the EPR spectral properties (g values, ^{55}Mn nuclear hyperfine couplings). Hence, all four multiline EPR signals are proposed to arise from an $s = {}^1/_2$ excited state, whereas the $g = 4.1$ EPR signal is proposed to arise from the $s = {}^3/_2$ ground state. A restriction that all five S_2 state species have an $s = {}^3/_2$ ground state and an $s = {}^1/_2$ first excited state seems warranted in view of the fact that all five EPR signals arise from the same paramagnetic site in the S_2 oxidation state. The calculations presented below, therefore, do not necessarily provide unique fits to the magnetic properties of all of the S_2 state EPR signals, but they do consolidate the available data into a self-consistent model of the Mn site in the S_2 state.

The Mn tetramer model discussed in the Theory section was employed to simulate the temperature-dependence behavior of all five EPR signals arising from the S_2 state of the OEC. The simulated curves are plotted against the experimental data in Figures 3 and 4, and the simulation parameters are tabulated in Table I. Values of $|D|$ ranging from 1.6 to 2.0 cm^{-1} were necessary to fit the breadth of the temperature-dependence curves, particularly those of the resting S_2 state multiline EPR signal produced by 200 K illumination and the active S_2 state multiline EPR signal produced by 245 K illumination. The moderately large values of $|D|$ also imply the existence of a strong axial crystal field around the Mn^{III} ions. Indeed, D is found to be large and negative in Mn^{III}–porphyrin complexes, where the porphyrin ring provides

(20) Moura, I.; Huynh, B. H.; Hausinger, R. P.; Le Gall, J.; Xavier, A. V.; Münck, E. J. *J. Biol. Chem.* **1980**, *255*, 2498.
(21) Weltner, W., Jr. *Magnetic Atoms and Molecules*; Scientific and Academic Editions: New York, 1983; p 241.
(22) Rutherford, A. W. *Biochim. Biophys. Acta* **1985**, *807*, 189.
(23) Richens, D. T.; Sawyer, D. T. *J. Am. Chem. Soc.* **1979**, *101*, 3681.

Table I. Parameters Used in the Simulation of the Temperature Dependence of the S_2 State EPR Signals

state of OEC	illumination (K)	D^a (cm^{-1})	J (cm^{-1})	J' (cm^{-1})	$\Delta_1{}^b$ (cm^{-1})	$\Delta_2{}^b$ (cm^{-1})
resting	130	2.0	48.0	−130.0	15.6	
		−1.0	48.0	−130.0	15.1	
	200	−2.0	53.0	−120.0	6.5	40.0
(NH_4Cl treated)	273	−1.6	23.0	−53.5	2.9	48.6
active	245	−2.0	23.0	−60.0	5.2	11.3
	160	−1.8	23.0	−54.5	3.2	14.3

$^a D = D_1 = D_2$; D_3 and D_4 do not enter into the calculations when a large antiferromagnetic superexchange coupling between Mn(III) and Mn(IV) is present. $^b \Delta_1$ is the energy separation in cm^{-1} between the $s = {}^3/_2$ level and the $s = {}^1/_2$ level; Δ_2 is the energy separation in cm^{-1} between the doulet giving rise to the signal and the next higher level.

Table II. Hyperfine Reduction Constants for a $3Mn^{III}$–Mn^{IV} Tetramer

state of OEC	illumination (K)	c_1	c_2	c_D	c_3	c_4
resting	200	−0.005	−0.006	−0.973	−1.946	0.973
(NH_4Cl treated)	273	−0.002	−0.002	−0.771	−1.542	0.771
active	245	0.010	0.010	0.120	0.240	−0.120
	160	−0.029	−0.029	−0.932	−1.864	0.932

the axial field.[24] We have, therefore, used negative values of D for the fits shown in Figures 3 and 4. The sign of D, however, has no effect on the eigenvalues of $\hat{H}_{zf}$ and, hence, does not influence the temperature dependence of the multiline EPR signals. The sign of D does determine which of the $s = {}^3/_2$ doublets, $m_s = \pm{}^1/_2$ or $m_s = \pm{}^3/_2$, is higher in energy, and this influences the temperature dependence of the transitions from the $s = {}^3/_2$ state.

It is noted that a satisfactory fit to the temperature behavior of the $g = 4.1$ S_2 state EPR signal can be accomplished by invoking a transition within the $m_s = \pm{}^1/_2$ levels of an $s = {}^3/_2$ state, with the $s = {}^1/_2$ state more than 15 cm^{-1} above it, as proposed above. It is possible to fit the Curie behavior of the $g = 4.1$ EPR signal with either sign of D. When D is positive, the $m_s = \pm{}^1/_2$ doublet is the ground state of the complex, and the data can be fitted with any moderately large value of D. A fit using $D = 2.0$ cm^{-1} is shown in Figure 3b (dashed line). When D is negative, the $m_s = \pm{}^1/_2$ doublet is higher in energy than the $m_s = \pm{}^3/_2$ doublet. In order to fit the temperature dependence of the $g = 4.1$ EPR signal, it is required that $|D| < 1.0$ cm^{-1}. A fit using $D = -1.0$ cm^{-1} is shown in Figure 3b (solid line). These two possibilities cannot be distinguished on the basis of our data.

The presence of an excited $s = {}^1/_2$ state above the $s = {}^3/_2$ state giving rise to the $g = 4.1$ EPR spectrum suggests that an EPR signal due to the excited $s = {}^1/_2$ state should be observed at higher temperatures in samples illuminated at 130 K. Illumination at 130 K produces an S_2 state species with a $g = 4.1$ EPR signal, but attempts to detect a multiline EPR signal at higher temperatures from this configuration of the Mn site have failed, perhaps due to line broadening which makes EPR measurements above approximately 20–30 K impossible. Conversely, one should also expect to observe, at sufficiently low temperatures, an EPR signal from the $s = {}^3/_2$ ground state of the resting S_2 state produced by 200 K illumination. We have thus far been unable, however, to detect any spectral features in the 0–10000-G range at 4.0 K which could be associated with the ground state of the Mn complex in samples illuminated at 200 K. An EPR signal from an $s = {}^3/_2$ state could be very difficult to detect, however, if the site does not have axial or higher symmetry, in which case the EPR spectrum would be very anisotropic.

The temperature dependence of the S_2 state multiline EPR signal from NH_4Cl-treated PSII membranes and the S_2 state produced by 160 K illumination of active state PSII membranes could be fitted by assuming a transition within the $s = {}^1/_2$ excited state. These two fits are shown in Figures 3c and 4a, respectively, and the parameters used in the simulation of the temperature dependences are listed in Table I. In order to account for the Curie behavior above 4 K, the energy separation between the $s = {}^1/_2$ and $s = {}^3/_2$ states was reduced, which required a reduction in $|J|$ and $|J'|$ relative to the values used to fit the temperature dependence of the resting S_2 state multiline EPR spectrum.

It is important to note that the coupling schemes of Table I accurately account for the microwave power saturation behavior of the EPR signals under discussion. In our earlier work,[6] we established the possibility that the resting and active S_2 state EPR signals relax via an Orbach mechanism, that is, via an interaction with an excited state of the spin system. For an Orbach mechanism, the microwave power at half-saturation, $P_{1/2}$, varies as $\exp(-\Delta_2/kT)$, where Δ_2 is the energy separation between the doublet giving rise to the EPR spectrum and the next higher excited state. A determination of Δ_2 was possible for the resting S_2 state multiline EPR signal ($\Delta_2 = 41.6$ cm^{-1}) and the active S_2 state multiline EPR signal produced by 160 K illumination ($\Delta_2 = 13.7$ cm^{-1}). The active S_2 state multiline EPR signal generated by 170 K illumination could not be saturated in the 4.0–10.0 K range,[6] thereby implying a low value of Δ_2, whereas the S_2 state multiline EPR signal of NH_4Cl-treated samples is more easily saturated than the resting S_2 state multiline EPR signal (data not shown), suggesting a high value of Δ_2. The values of Δ_2 listed in Table I account for these data. This model can, therefore, account for the magnetic properties of all five EPR signals from the S_2 state of the OEC.

The Mn tetramer model can also explain the ^{55}Mn nuclear hyperfine features of the S_2 state multiline EPR signals. For each S_2 state multiline EPR signal, the hyperfine reduction constants of each ion in the tetramer are shown in Table II. The eigenfunctions of the ($s = {}^1/_2$, $m_s = +{}^1/_2$) and ($s = {}^1/_2$, $m_s = -{}^1/_2$) states were obtained by diagonalization of $\hat{H}_{zf}$, using the parameters of Table I. The procedures outlined in the Theory section were then followed in order to determine the hyperfine reduction constants. The large values of c_D found for both resting state multiline EPR signals (untreated and ammonia-bound) and the active S_2 state multiline EPR signal produced by 160 K illumination indicate that these spectra have much Mn^{III}–Mn^{IV} dimer character. The active S_2 state multiline EPR spectrum produced by 245 K illumination, however, exhibits a low value of c_D due to mixing of the $s = {}^1/_2$ and $s = {}^3/_2$ states, thus suggesting more tetramer character in the spectrum. Furthermore, the reduction in c_D from −0.973 to −0.771, or 21%, which results from the addition of NH_4Cl to resting state membranes, parallels the reduction by 23% in the average separation of the hyperfine lines of the S_2 state multiline EPR spectrum upon NH_4Cl treatment.[7]

The conclusion that the ^{55}Mn nuclear hyperfine interaction in the resting S_2 state EPR spectrum can be reasonably described by a Mn dimer suggests that, even though the explanation of the magnetic properties requires a tetramer model, a computer simulation of the resting S_2 state multiline EPR spectrum can be achieved with an antiferromagnetically exchange coupled Mn^{III}–Mn^{IV} dimer model. This has been attempted by Hansson and Andrēasson[14] and Dismukes and Siderer.[8] Their simulated spectra, however, failed to accurately reproduce the intensity pattern of the hyperfine lines in the S_2 state multiline EPR

(24) Brackett, G. C.; Richards, P. L.; Caughey, W. S. *J. Chem. Phys.* **1971**, *54*, 4383.

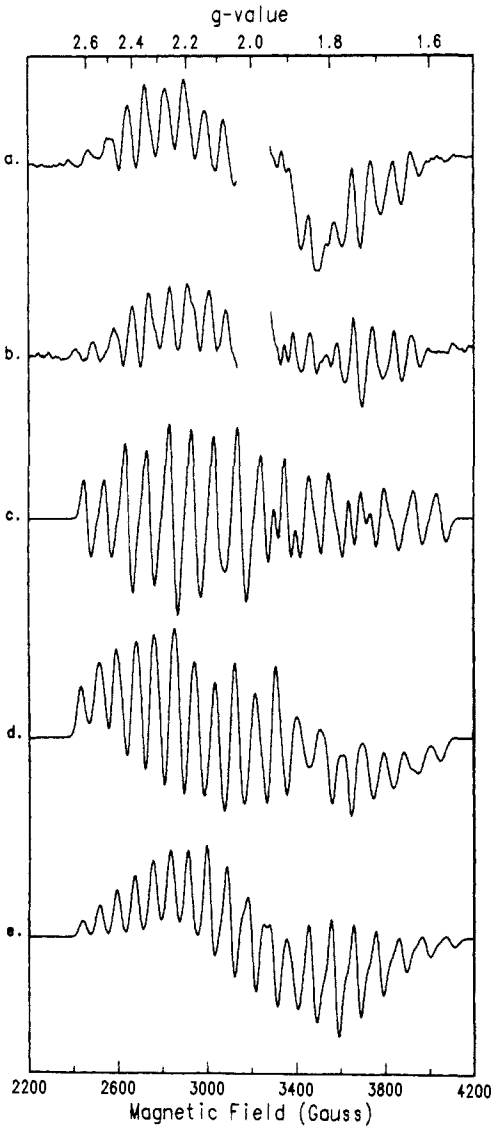

Figure 5. Comparison between the experimental and calculated resting S_2 state EPR spectra. (a) 200 K illuminated minus dark PSII; (b) 200 K illuminated then incubated at 0 °C for 1 min minus dark PSII treated with 250 μM DCBQ. Calculated spectra (ν = 9.10 GHz): (c) g^c = 1.98, A_1^c = 0.0200 cm^{-1}, A_2^c = −0.00930 cm^{-1}; (d) g_x^c = 1.930, g_y^c = 2.004, g_z^c = 2.100, A_1^c = 0.0170 cm^{-1}, A_2^c = −0.0080 cm^{-1}; (e) g_x^c = 1.810, g_y^c = 1.960, g_z^c = 2.274, A_1^c = 0.0086 cm^{-1}, A_2^c = −0.0086 cm^{-1}.

spectrum, particularly the weak intensity of the lines at low and high magnetic fields. In these earlier calculations, isotropic **g** and **A** tensors were assumed. We advance the possibility that the past lack of success in simulating the S_2 state EPR spectrum was due to the assumption that the **g** tensor of the dimer is isotropic.

The simulation of the S_2 state multiline EPR signal is made difficult by the existence of other EPR signals from PSII components in the 2200–4200-G region of the EPR spectrum. Difference spectroscopy partially alleviates this problem by subtracting away background contributions which are not light-induced. The EPR signal II contribution at g = 2.0, however, cannot be easily subtracted out due to the dynamic range of the digitization. Figure 5a shows that, aside from the EPR signal due to the Mn site in the S_2 state, a broad EPR signal centered at $g \sim 1.9$ is also observed. This g = 1.9 EPR signal is known to arise from the reduced electron acceptor Q_A of PSII, which is magnetically coupled to a Fe^{II} ion.[25] The presence of the Fe^{II}–Q_A^- EPR signal obviously renders fitting of the position and intensity of the hyperfine lines of the S_2 state multiline EPR signal difficult for the portion of the spectrum near g = 1.9. We have eliminated this interference at $g \sim 1.9$ by performing the following experiment. The electron acceptor 2,5-dichloro-*p*-benzoquinone (DCBQ) was added at a concentration of 250 μM to a sample of dark-adapted PSII membranes. Following illumination at 210 K, the sample was incubated in the dark for 1 min at 0 °C. This allowed Q_A^- to be oxidized by DCBQ, whereas the S_2 state multiline EPR signal intensity was reduced by only ~10% due to back-reaction. Figure 5b shows that, indeed, the Fe^{II}–Q_A^- EPR signal centered at $g \sim 1.9$ was lost as a result of the brief incubation at 0 °C. It is also noted that no changes in line positions of the S_2 state multiline EPR signal were observed upon dark incubation at 0 °C.

The method outlined in the Theory section was used to simulate the S_2 state multiline EPR spectrum. Figure 5c shows that the use of an isotropic g value of 1.98 and inequivalent Mn ions afforded a poor fit to the experimental spectrum. Noteworthy is the fact that the decrease in intensity observed in the low and high field extremes of the experimental spectrum is not reproduced in the calculation. Furthermore, the values of A_i' used to simulate the breadth of the EPR spectrum were unreasonably larger than those which are expected for Mn^{III} or Mn^{IV}.[26] In Figure 5d, an attempt is made to remedy the problem by introducing anisotropy in the **g** tensor. The values of A_i' were chosen to fall within the range expected for Mn^{III} and Mn^{IV}, i.e., A_i' = 0.0070 − 0.0090 cm^{-1}. Although it is possible to more closely match the positions of the hyperfine lines in this case, the intensities cannot be well reproduced. In particular, the low-field portion of the experimental spectrum does not cross below the base line, and this feature could not be reproduced in the calculations using an anisotropic **g** tensor when the Mn ions are inequivalent. Figure 5e shows a simulation of the S_2 state multiline EPR signal where the Mn ions are assumed to be equivalent, i.e., the values of A_i' were chosen so that $2|A_1^c| = |A_2^c|$. Such an equivalence requires rapid electron exchange between the Mn^{III} and Mn^{IV} ions on the EPR time scale. The positions and intensity pattern of the hyperfine lines to low field of g = 2.0 are very accurately reproduced by this simulation. Although the hyperfine line positions to high field of g = 2.0 are accurately reproduced in Figure 5e, their intensities are not well fit in this region of the spectrum. The high-field lines may show better agreement with the experimental spectrum if anisotropy is included in the nuclear hyperfine coupling tensor.

The inclusion of g anisotropy in the Mn^{III}–Mn^{IV} model for the S_2 state of the OEC has experimental precedent. Rutherford[22] has studied the S_2 state EPR signal obtained by 200 K illumination of PSII membranes and found that the lowest field lines of the spectrum exhibited considerable orientation dependence. He did not investigate the behavior of the lines to high field of g = 2.0, since these suffer from interference from orientation-dependent EPR signals from the electron acceptor side of PSII. Our interpretation of the S_2 state multiline EPR spectrum predicts that the lowest and highest field lines of the spectrum, which arise from g_z and g_x contributions, respectively, should exhibit the best defined orientation dependence. The lines closer to g = 2.0 have overlapping contributions from g_x, g_y, and g_z which obscure the orientation dependence in this region. We are currently engaged in a more complete investigation of the orientation dependence of all five S_2 state EPR signals. Finally, we note that g anisotropy can explain the existence of a broad Gaussian component which lies underneath the main hyperfine lines of the S_2 state multiline EPR signal (Figure 5b). The presence of this Gaussian component causes the hyperfine lines in the low-field portion of the spectrum to not cross below the base line. As can be observed in Figure 5e, this Gaussian component is a direct consequence of the merging of lines from the three different turning points of the spectrum. Hansson et al.[27] found that subtracting an arbitrary amount of a Gaussian line from the S_2 state multiline EPR spectrum was

(25) Rutherford, A. W.; Zimmermann, J. L. *Biochim. Biophys. Acta* **1984**, *767*, 168.

(26) Abragam, A.; Bleaney, B. *Electron Paramagnetic Resonance of Transition Ions*; Clarendon Press: London, 1970.

(27) Hansson, Ö.; Andréasson, L.-E.; Vänngård, T. *Advances in Photosynthesis Research*; Sybesma, C., Ed.; Nijhoff/Junk Publishers: The Hague, 1984; Vol. 1, p 307.

required for agreement between their observed and calculated spectra. Our conclusion that this Gaussian feature is an integral part of the S_2 state multiline EPR spectrum, and not due to background interference, is further supported by our observation that it exhibits the same temperature dependence and microwave power saturation behavior as the sharper features of the spectrum (data not shown).

It is important to point out that a Mn^{III}–Mn^{IV} dimer model can only be successful in simulating the EPR spectrum of the S_2 state produced from the untreated resting state by 200 K illumination. The results of Table II show that the other S_2 state multiline EPR signals have considerable tetramer character and, consequently, the Mn^{III}–Mn^{IV} dimer approximation of the ^{55}Mn nuclear hyperfine coupling becomes invalid.

Conclusions

In this contribution, we advance a model for the S_2 state of the OEC where two antiferromagnetically exchange coupled Mn dimers are ferromagnetically exchange coupled. Both the magnetic properties and the ^{55}Mn nuclear hyperfine couplings of five distinct S_2 state EPR signals can be satisfactorily explained by this model.

The simulation parameters in Table I indicate that both large antiferromagnetic and ferromagnetic exchange couplings are needed to explain the temperature dependence and microwave power saturation behavior of the S_2 state EPR spectra. Even though large ferromagnetic exchange couplings are not commonly found in synthetic complexes, a few examples do exist.[18] There is also ample precedent in the literature of tetrameric complexes where both large antiferromagnetic and large ferromagnetic exchange interactions occur simultaneously, such as Cu_4O_4 cubane-like clusters[13] and the Fe_4S_4 centers of ferredoxins.[12] The analogies which can be made with the Cu_4O_4 and Fe_4S_4 cubane-like complexes prompt us to speculate that the Mn site of the OEC exists as a Mn_4O_4 cubane-like structure in the S_2 state.

Acknowledgment. This work was supported by the National Institutes of Health (GM32715), the Chicago Community Trust/Searle Scholars Program, the Camille and Henry Dreyfus Foundation, and a National Science Foundation Graduate Fellowship to W.F.B.

Transient Photoligation Behavior of Nickel Protoporphyrin Reconstituted Myoglobin and Hemoglobin†

E. W. Findsen,‡ K. Alston,§ J. A. Shelnutt,⊥ and M. R. Ondrias*†

Contribution from the Department of Chemistry, University of New Mexico, Albuquerque, New Mexico 87131, Department of Natural Sciences, Benedict College, Columbia, South Carolina 29204, and the Solid State Materials Division, Sandia National Laboratories, Albuquerque, New Mexico 87185. *Received January 9, 1986*

Abstract: The transient photoligation behavior of nickel protoporphyrin IX (Ni(PP)) in a variety of local environments has been studied by time-resolved resonance Raman scattering. In coordinating basic solvents the ligation changes engendered by the photoexcitation of a net $d^2_{z^2} \rightarrow d^1_{x^2-y^2}, d^1_{z^2}$ ($^1A_{1g} \rightarrow {}^3B_{1g}$) transition are easily monitored by changes in Ni(PP) Raman modes that are sensitive to metalloporphyrin spin-state and ligation changes. The Raman results for those systems corroborate the photochemical cycle and excited state lifetimes proposed by Holten and co-workers (*Chem. Phys.* **1983**, *75*, 305). However, the photodynamics exhibited by Ni(PP) incorporated into Mb or Hb apoproteins or into detergent micelles are distinct from those of Ni(PP) in coordinating solvents and from each other. The equilibrium 4-coordinate Ni(PP) sites in NiHb display a transient photoassociation of a single ligand (most likely the proximal histidine) similar to the behavior of Ni(PP) in solution. The photodynamics of the equilibrium 5-coordinate Ni(PP) sites in NiHb and NiMb are, however, greatly modulated by the surrounding protein matrix. The major effects of the protein environment are concluded to be the stabilization of the ligand binding transition states thus facilitating photoassociation of the proximal histidine at the 4-coordinate site and enhancing the recombination rate of the photodissociated histidine at the 5-coordinate sites. In a hydrophobic micellar environment where no potential axial ligands are present, photoexcitation of 4-coordinate Ni(PP) results in the direct observation of the resonance Raman spectrum of the unligated $^3B_{1g}$ state. This allows for the deconvolution of the effects upon the porphyrin of the excited-state spin-state transition from those produced by ligation.

The metalloporphyrins are a diverse class of complex molecules that display a wide variety of photochemical and metal ligand binding behavior.[1-3] They are of interest as potential catalysts and photosensitizing agents as well as for understanding the key role that metalloporphyrins play in biological processes. Moreover, the chemical properties of specific metalloporphyrins are significantly altered when they are incorporated into a protein matrix. The pervasive influence of the protein environment upon the equilibrium properties of metalloporphyrin active sites is well-documented for a wide variety of systems.

Recently, transient optical techniques have demonstrated that the dynamic behavior of active sites in hemoproteins is similarly predicted to a large degree upon its immediate protein environment.[4-7] Transient resonance Raman scattering has proven

† This work was performed at the University of New Mexico and supported by the National Institutes of Health (GM33330), the donors of the Petroleum Research Fund, administered by the American Chemical Society (to M.R.O.), The U.S. Department of Energy (Contract DE-AC04-76DP00789), the Gas Research Institute (Contract No. 5082-260-0767 (to J.A.S.)), and the graduate research scholarship fund of the Associated Western Universities (to E.W.F.).

‡ University of New Mexico.
§ Benedict College.
⊥ Sandia National Laboratories.

(1) *The Porphyrins*; Dolphin, D., Ed.; Academic Press: New York, 1978–1983; Vol. 1–8.
(2) *Iron Porphyrins*; Lever, A. B. P., Gray, H. B., Eds.; Addison-Wesley: Reading, PA, 1983; Vols. 1 and 2.
(3) *Porphyrins and Metalloporphyrins*; Smith, K. M., Ed.; Elsevier: New York, 1975.
(4) Friedman, J. M.; Ondrias, M. R.; Rousseau, D. L. *Annu. Rev. Phys. Chem.* **1982**, *33*, 471.
(5) Spiro, T. G. In *Iron Porphyrins*; Lever, A. B. P., Gray, H. B., Eds.; Addison-Wesley: Reading, PA, 1983; Vol. 2, p 89.
(6) Debunner, P. G.; Frauenfelder, H. *Annu. Rev. Phys. Chem.* **1982**, *33*, 283.

0002-7863/86/1508-4009$01.50/0